Design of Scramjet Inlet for Shock on Lip Condition at Low Mach Number by Using CFD

Ganesh Borde
Department of Aeronautical Engineering
Vel Tech Rangarajan Dr. Sagunthala R&D Institute of Science and Technology
Chennai, INDIA
ganeshyng789@gmail.com

Naren Shankar R
Department of Aeronautical Engineering
Vel Tech Rangarajan Dr. Sagunthala R&D Institute of Science and Technology
Chennai, INDIA
rnarenshankar@gmail.com

***Abstract* - In the new era of technology, the Scramjet engine has a big future in both Supersonic and Hypersonic flights. Flow at hypersonic Mach numbers acts in a completely different way than flow at subsonic or supersonic Mach numbers, because air combustion occurs at supersonic speeds, the airflow is compressed from hypersonic to supersonic. A profile of the inlet allows for the decrease of this speed. The project deals to develop a two-dimensional inlet geometry that can function at Mach 4 and 5 without causing flow spillage in the engine, because flow spillage creates drag. This is accomplished by establishing a shock on lip phenomenon, in which all inlet ramp shocks pings at the cowl tip and are reflected back to the isolator. By forming a shock train, this shock is constantly reflected back to the isolator. The compression of airflow at the entry of the combustion chamber at these speeds does not achieve high temperature. As a result, hydrocarbons fuel JP-7is used for combustion, which has ignition temperature of 514.15K. The geometry of the inlet is calculated by using the theoretical equation for getting the maximum total pressure ratio. To determine appropriate inlets for M4 and M5, Numerical analysis are used for finding of pressure, temperature, and Mach number.**

Keywords- Shock on lip, Ignition Temperature, Drag, Spillage of flow, Cowl tip, shock train.

I. INTRODUCTION

A scramjet, or supersonic combustion ramjet, is a development of the ramjet engine in which combustion takes place at supersonic rather than subsonic speeds. The air passes through narrow slit open which results in increase of temperature and pressure. The combustion takes place by just injection of fuel which in turn increases the enthalpy of flow and expands through the divergent nozzle leading to high acceleration of flow and creating the thrust. The scramjet consists of four major parts namely, inlet, isolator, combustion chamber, and expansion nozzle as shown in the Fig. 1. The inlet is very critical part of the entire design, because its seamless profile bends the air which produces shock waves and decides the proper compression. Imperfection in inlet profile can lead to unstart of the engine. Commonly there are three types of inlets design which can achieve compression. They are external compression, mixed compression and internal compression. The best method for compression is mixed compression inlet is shown in the Fig. 2. Here the compression is performed by shocks both external and internal to the engine conduct compression here, and the angle of the exterior cowl relative to the freestream can be made very small to reduce external drag. There inlets are often longer than external compression configurations. The purpose of an isolator, which is a short duct located between the inlet and combustion chamber of a scramjet engine, is to isolate approaching flow and prevent interaction between the combustion and inlet, hence reducing flow perturbations induced by the combustion process.

The shock on lip is a condition where all oblique shock from the engine ramp gets impinge at the tip cowl and gets reflected to isolator as shown in Fig. 3. This is generated in a mixed compression type inlet. This phenomenon creates no

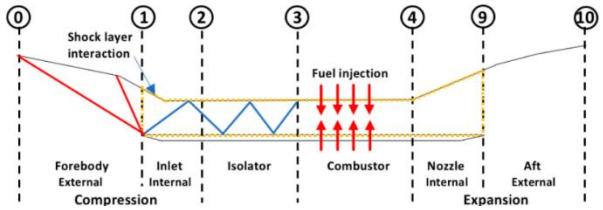

Fig. 1. Two-dimensional schematic of a scramjet engine [1]

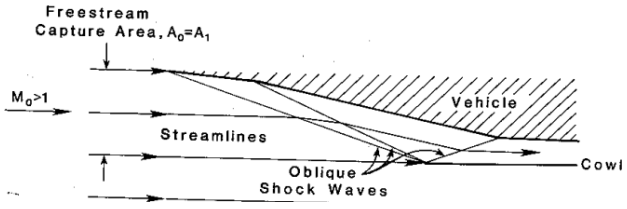

Fig. 2. Mixed compression [2]

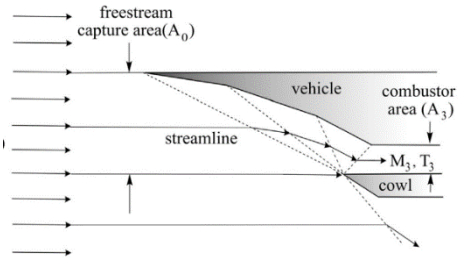

Fig. 3 Shock on Lip Condition

mass spillage for the engine and reduces drag in the engine i.e., cowl wave drags. As we have seen a reduction in drag means the fuel consumption of the engine is also less.

During the 1950s and 1960s, significant study revealed that if we want to eliminate the restraints of rockets while also increasing performance, Scramjet or air-breathing propulsion is a viable choice to a rocket. The flight corridor for scramjet-powered vehicles to cruise or ascend to low-Earth orbit. Hypersonic airbreathing flight corridor depicts these constraints and includes a proposed ascent trajectory for an airbreathing access-to-space vehicle, which features turbojet operation up to Mach 3-4 and scramjet operation [3]. Fry [4] explains the efficient operating Mach number range for different propulsion systems with two fuel options: hydrogen and hydrocarbons. Heiser and pratt [2] described how to evaluate the freestream condition of the flow, a constant dynamic pressure (q) trajectory is applied which provides the corresponding velocity, altitude, temperature, pressure., the ratio of specific heats at constant pressure. And also, to evaluate the Mach number and temperature at the entrance of the combustion chamber. Mach number at the inlet exit is a function of the flight Mach number. Anderson [5] has explained the theory of oblique shock for inviscid flow. The flow properties (such as pressure, temperature, Mach number and density) after each shock are calculated by using oblique shock relation.

They are Numerous research on designing scramjet demonstrator engine, where their inlet type is wedge or plane waverider, with different types of compression methods i.e., external, internal and mixed compression. Several optimization methods for design of scramjet inlets bases on temperature and Mach number at the entry of combustion chamber, after the reflected shock in isolator. Using gas dynamics relations and Lagrange multipliers Oswatitsch [6] developed an optimal design for supersonic inlet, reduces the supersonic freestream air to subsonic in combustion chamber. In order to achieve maximum total pressure ratio, a set of n-1 oblique and one normal compression shock for a given Mach number of the flow were obtained. To get maximum compression efficiency oblique shock must generate equal strength. Prakash and Venkatasubbaiah [7] have developed a new methodology for design pf scramjet inlet by using gas dynamic relations. Inlet geometry has designed such that it has maximum total pressure recovery at designed free stream Mach number and Shock on lip condition which avoids flow spillage. Designed inlet performance are calculated by using CFD analysis. Araújo et.al. [8] presented a 2D mixed compression scramjet inlet design based on temperature and Mach number at combustion inlet condition required to burn fuel at supersonic speeds by considering air as perfect gas, no viscous effects and shock on lip condition. To determine the compression ramp angles and the airflow corresponding thermodynamic properties, the equal shock strength criterion is used. It is based on the normal component of the airflow velocity approaching the incident oblique shock waves. Concluded that by varying the number of ramps from 1 to 5, the total pressure ratio at the external compression section increases and the total pressure ratio at the internal compression section decreases.

Roberts and Wilson [9] the aim of research is to check whether the starting Mach number of 2D scramjet engine can be lowered to 3.50. They observed that scramjet inlet with starting Mach number 3.50, the temperature in combustion chamber was lower than ignition temperature (IT) of fuel. However, a scramjet with a starting Mach number of 4.00 has achieved the temperature in combustion chamber was higher than IT of fuel. The geometry parameters of engine design are calculated by using relations from Heiser and pratt [2]. Karthikeyan et.al. [10] objective is to lower starting Mach number of scramjet, which enables use of two propulsion systems to complete the entire mission and also enables a reduction in overall weight of the system. To operate at range of Mach numbers, they analysed geometry by varying moment of cowl lip. Concluded that vertical movement of cowl lip geometry showed better result than forward moment of cowl lip. Zore et.al. [11] presents the hypersonic flow simulations carried out using ANSYS Fluent, including the use of mesh adaptation techniques to achieve fast, robust, and accurate solutions. For a 2D wedge at Mach number 5 For this case, wall pressure, skin-friction coefficient and mean-flow boundary layer profiles, before/aftershock impingement shows good agreement with the experimental data.

The existing programs for scramjet engine, they all are operated at a higher Mach number i.e., above Mach 6. They require a rocket booster to attend the flight Mach number and they use Hydrogen fuel it has a high ignition temperature (IT) i.e., 845°K as shown in Table 1. So, the aim to design the scramjet to work in lower speed i.e., Mach 4 and Mach 5 and with minimal variable geometry features and the use of hydrocarbon fuel. SR-71 blackbird turbojet engine can provide thrust from take-off to a speed of Mach 3 or 4. Therefore, if a scramjet were designed with a starting Mach number of about 4, presumably only two propulsion systems would be needed for the entire mission since our main objective of this project is to “enable sustained hypersonic flight for missile or aircraft applications and to develop and demonstrate Mach 4 and Mach 5 hydrocarbon-fuelled. And also, the use of phenomena of shock on lip condition reduces the flow spillage and the cowl drag. So, if less drag is created then we have less fuel consumption. For Mach number 4 and 5 the temperature achieved by compressing the freestream by inlet exit is between range of 600°K to 900°K.Hydrogen is not used fuel because it has IT of 845.15°K. So, JP-7 fuel is used, since it has ignition temp of 514.15°K [12].

Table 1. Ignition temperature (IT) of fuels

Fuel	**IT(K)**
Hydrogen	845.15
JP-7	514.15

II. METHODOLOGY

Freestream condition of the flow are determined by using a constant dynamic pressure (q)value of 47,880 N/m^2 [2], which uses standard atmosphere properties, the freestream Mach number, and the value of dynamic pressure input to calculate a constant- q trajectory and provides the corresponding velocity, altitude, temperature, and pressure for the freestream Mach number which are tabulated in Table 2 for Mach number 4 and 5.

Table 2. Freestream of air at Mach 4 and 5

q	477880 N/m^2				
γ	1.4				
C_{pc}	1006 J/KgK				
M_0	**V_0**	**H**	**H**	**T_0**	**p_0**
	m/s	m	km	K	Pa
4	1184.56	21646.90	21.65	218.22	4275
5	1490.40	24539.45	24.54	221.09	2736

A. Scramjet Inlet Design

The main parameter for designing a scramjet engine is temperature before the combustion chamber i.e., T_3 means the temperature at which combustion takes place. The fuel JP-7 is used for combustion, since it is hydrocarbon fuel which as lower IT, these values are taken from Roberts and Wilson [9]. The values of temperature ratio are given in Table 3 for Mach 4 and 5, they are calculated such that the Mach number in before combustion (M_3) should not lead to 1. A "special family" can be designed by using HAP (Gas Tables) [2] by inputting M_0 and T_3/T_0. The number of oblique shock waves has a direct impact on the compression efficiency (η_c); a good estimate of this correlation can be seen in Fig. 4. It should be noted that the higher the number of oblique shock waves, the longer the compression system will be. Also, with more oblique shocks, more off-design complications. It is observed that for designed temperature ratio required for combustion for Mach number 4 and 5. It was found that compression efficiency was about 0.90 and the number of shocks generated are 3. The general overview of ramps and shock is given in Fig.5.

Table 3. Temperature ratios for Mach 4 and 5

Mach number	***ψ***
4	2.80
5	3.75

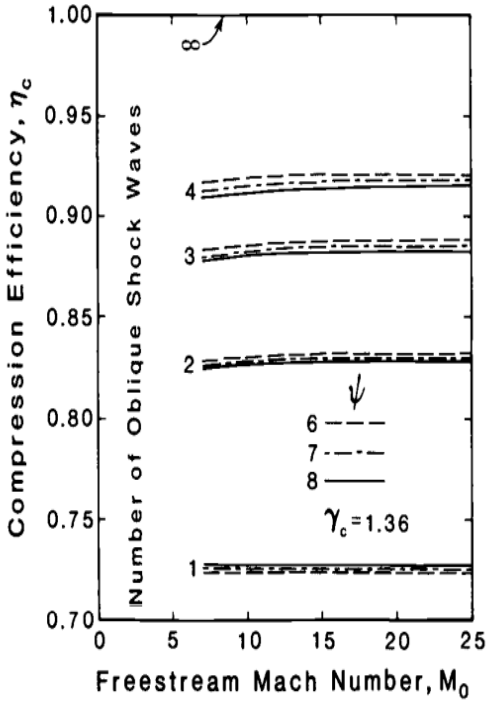

Fig. 4 Compression Efficiency Correlated to M_0 , T_3/T_0, and Number of Oblique Shock Waves [2]

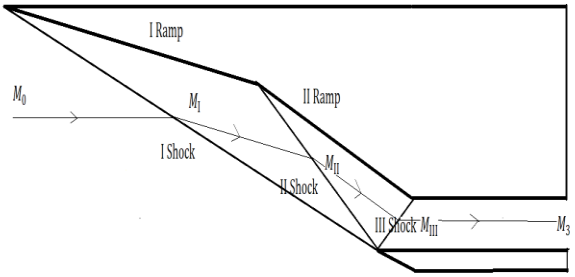

Fig. 5 Shock structure for 2 ramp scramjet inlets

Area ratio is the ratio of the area of capture area to isolator area. The procedure to find Area ratio is given below. The values T_0, M_0, V_0 , γ_c and C_{pc} for Mach number 4 and 5 are taken from Table 2. Combustion entry Temperature

$$\psi = \frac{T_3}{T_0}$$

$$T_3 = \psi \times T_0$$

For M4 inlet

$T_3 = 2.80 \times 218.22$

$= 611.016$ K

For M5 inlet

$T_3 = 3.75 \times 221.09$

$= 829.087$ K

Combustion entry Mach number

$$M_3=\sqrt{\frac{2}{\gamma_c-1}\left\{\frac{T_o}{T_3}\left(1+\frac{\gamma_c-1}{2}M_o^2\right)-1\right\}}$$

For M4 inlet

$$M_3=\sqrt{\frac{2}{1.4-1}\left\{2.80\left(1+\frac{1.4-1}{2}16\right)-1\right\}}=1.581$$

For M5 inlet

$$M_3=\sqrt{\frac{2}{1.4-1}\left\{3.75\left(1+\frac{1.4-1}{2}25\right)-1\right\}}=1.732$$

Combustion entry Velocity

$$V_3=\sqrt{V_0^2-2C_{pc}T_0(\psi-1)}$$

For M4 inlet

$$V_3=\sqrt{1184.561^2-2\times1006\times218.22\times(2.80-1)}$$

$=782.679$ m/s

$$\frac{V_0}{V_3}=1.513$$

For M5 inlet

$$V_3=\sqrt{1490.40^2-2\times1006\times221.09\times(3.75-1)}$$

$=996.910$ m/s

$$\frac{V_0}{V_3}=1.495$$

Total pressure ratio

$$\pi_c=\left\{\frac{1}{\psi(1-\eta_c)+\eta_c}\right\}^{\gamma_c/(\gamma_c-1)}$$

For M4 inlet

Considering η_c =0.90, ψ =2.80

$$\pi_c=\left\{\frac{1}{2.80(1-0.90)+0.90}\right\}^{1.4/(1.4-1)}=0.560$$

For M5 inlet

Considering η_c =0.90, ψ =3.75

$$\pi_c=\left\{\frac{1}{3.75(1-0.90)+0.90}\right\}^{1.4/(1.4-1)}=0.427$$

Static pressure ratio

$$\frac{p_3}{p_0}=\left\{\frac{\psi}{\psi(1-\eta_c)+\eta_c}\right\}^{\gamma_c/(\gamma_c-1)}$$

For M4 inlet

$$\frac{p_3}{p_0}=20.580$$

$$p_3=87983.695\,\frac{N}{m^2}$$

For M5 inlet

$$\frac{p_3}{p_0}=43.633$$

$$p_3=119382.281\,\frac{N}{m^2}$$

Area ratio of inlet

$$\frac{A_3}{A_0}=\psi\frac{p_0}{p_3}\frac{V_0}{V_3}$$

For M4 inlet

$$\frac{A_3}{A_0}=2.80\times\frac{1}{20.580}\times1.513$$

$$\frac{A_3}{A_0}=\frac{h_0}{h_3}=0.205$$

For M5 inlet

$$\frac{A_3}{A_0}=3.75\times\frac{1}{43.633}\times1.495$$

$$\frac{A_3}{A_0}=\frac{h_0}{h_3}=0.128$$

The aim of the project is to design geometry with a 1000 mm capture area, taking h_0=1000 mm [9]. Using a criterion for getting maximum pressure ratio by keeping equal shock strength between all shocks the relation (1). A sketch of parameters for design of geometry are shown in Fig. 6. Calculating all the parameters by using the Θ-β-M relation [5]. Using trial-and-error Method it found that θ_I lies between 10° and 12°. The specification of geometry is calculated by using inviscid theory, to perform analysis in viscous flow i.e., real flow analysis, so the position of the cowl changed by 25mm downwards. This value is found by interpolating CFD solution between inviscid solution and viscous solution. The area ratio of the inlet is kept the same. The specification of inlet geometry for Mach number 4 and 5 in Table 4 and 5.

$$M_0 \sin \beta_I = M_I \sin \beta_{II} \quad (1)$$

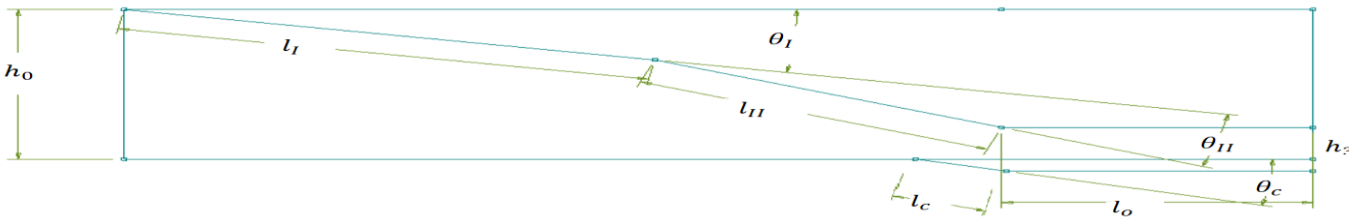

Fig. 6 Sketch of geometry specification

Table 4. Geometry parameters for M4 inlet for Inviscid theory and viscous effects

	Inviscid Theory				**Viscous Effects**			
θ_I	10	10.5	10.75	10.85	10	10.5	10.75	10.85
h_0 [mm]	1000	1000	1000	1000	1025	1025	1025	1025
l_I [mm]	1503.582	1518.907	1525.608	1528.117	1503.582	1518.907	1525.608	1528.117
θ_{II}	12.036	12.767	13.139	13.288	12.036	12.767	13.139	13.288
l_{II} [mm]	1420.630	1309.559	1258.250	1238.458	1473.542	1359.816	1307.273	1287.005
θ_c	10	10.5	10.75	10.85	10	10.5	10.75	10.85
l_c	356.741	310.000	289.415	281.655	406.545	356.955	335.039	326.764
l_o [mm]	2058.846	2058.846	2058.846	2058.846	2110.317	2110.317	2110.317	2110.317
h_3 [mm]	205.884	205.884	205.884	205.884	211.031	211.031	211.031	211.031

Table 5. Geometry parameters for M5 inlet for Inviscid theory and viscous effects

	Inviscid Theory				**Viscous Effects**			
θ_I	10	10.5	11	11.25	10	10.5	11	11.25
h_0 [mm]	1000	1000	1000	1000	1025	1025	1025	1025
l_I [mm]	1899.145	1901.831	1904.003	1904.107	1899.145	1901.831	1904.003	1904.107
θ_{II}	12.476	13.208	14.017	14.419	12.476	13.208	14.017	14.419
l_{II} [mm]	1473.792	1300.579	1197.339	14.419	1474.348	1360.047	1253.894	1198.372
θ_c	10	10.5	11	11.25	10	10.5	11	11.25
l_c	394.675	294.789	270.149	241.971	395.196	350.166	310.294	284.377
l_o [mm]	1304.847	1304.847	1304.847	1304.847	1315.740	1315.740	1315.740	1315.740
h_3 [mm]	130.484	130.484	130.484	130.484	131.574	131.574	131.574	131.574

B. *Numerical Analysis*

The Reynolds Average Navier-Stokes (RANS) equations are a decomposition of the Navier-Stokes equations into the time-averaged, and fluctuating component. The two-equation Shear-Stress-Transport (SST) k-ω model combines the robustness and accuracy of the k-ω model at the near-wall region with the freestream independence of the k-ϵ model away from the surface. The SST model is more accurate and reliable for a wider class of flows. Ansys Fluent software is used for Numerical solution. Density-based solver is chosen, in the compressible flow, pressure is a function of both density and temperature and for incompressible flow, pressure-based solvers are used because it was created for high-speed compressible flows. The steady flow has chosen because point of interest is the identification of oblique shock wave propagation. In Fluid properties, ideal gas air is chosen as fluid material. The density of air is chosen as ideal gas. Equation (2) is used to density, by using the pressure and temperature at specific condition. The viscosity is calculated by Sutherland law (3) [13], The boundary conditions are assigned as shown in Fig. 7. The inlet is taken as pressure farfield, with free-stream Mach number and static conditions being specified. The pressure far-field boundary condition is often called a characteristic boundary condition. It is applicable only when using the ideal- gas law. Under operating condition, the operating pressure is set to 0 Pa. Therefore, the inlet pressure directly matches given wind tunnel pressure data. The outlet conditions are identical to the inlet conditions. However, for this simulation, it does not matter what the outlet conditions are, because for locally supersonic flow the pressure is extrapolated from the upstream conditions. The walls of inlet geometry are taken as adiabatic condition. An implicit method is more efficient in cases when the time step can be increased beyond the explicit method, because the time scales of the main flow perturbations are large. This allows for larger time steps to be solved and still give an accurate solution. The Advection Upstream Splitting Method (AUSM) is chosen as the numerical flux function. It has many beneficial features such as providing exact resolution of the shock discontinuities and is also free of oscillations at stationary and moving shocks. This method is computationally less expensive than node-based gradient methods. 2nd Order Upwind is chosen for all other spatial discretization terms. The solution is initialized by hybrid initialization. Calculations ran for 2000 iterations when residuals converged and monitored variables settled.

$$p=\rho R_{specific}\, T \tag{2}$$

$$\mu=\mu_{ref}\left(\frac{T}{T_{ref}}\right)^{3/2}\frac{T_{ref}+S}{T+S} \tag{3}$$

C. *Grid independency study*

The meshing for geometry is done by using “Ansys Fluent Meshing” software. Structured Meshing technique used, because the quality of that grid plays a critical role in the overall analysis. This technique typically allows the user better control of interior node locations and sizes as interior node placement is directly linked to the user-defined exterior nodes. The grid generation of inlet design is shown in Fig. 8. Generally, a denser mesh is preferred and more desirable for capturing flow property fluctuations. However, a very fine mesh or dense mesh requires significantly larger computational resources and time. As the level of the fineness is further increased, the refinement effect on numerical results is diminished, and beyond a certain level of the fineness, vast computational resources are spent on negligible refinement effect. A compromise is found by conducting this grid independence study for inviscid flow up to only the inlet section as shown in Fig. 9 for a coarse grid of 30246, a medium grid of 119396 and the fine grid of 375191. The difference between the medium and fine meshes is not significant. To save computational resources, the mesh with a medium level of fineness is chosen.

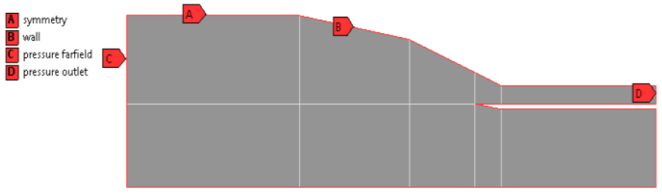

Fig. 7 Boundary condition for CFD domain

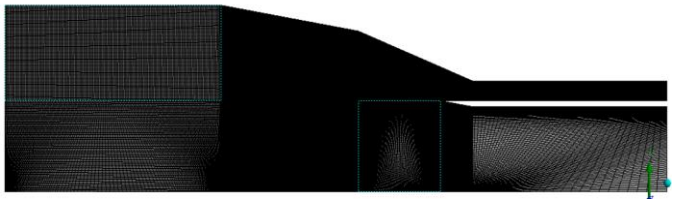

Fig. 8 Meshing of the geometry

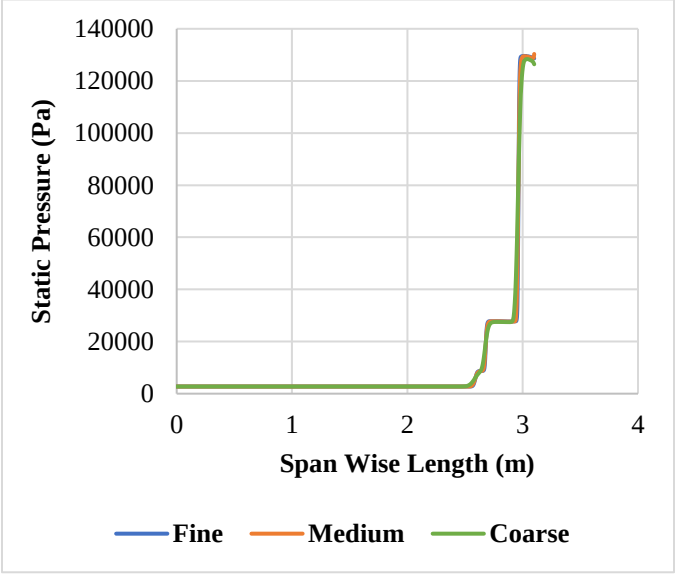

Fig. 9 Graph of Grid independence Study

III. Result and Discussion

Only a few research papers have utilized FLUENT to simulate hypersonic flow, and even fewer have validated it with experimental data. The Setup is validated from the experimental values taken from Neuenhahn and Olivier [14]. The boundary condition for the validation is static pressure as 5.2 mbar, static temperature 106°K, Mach number 8.1 and density is calculated by ideal gas rule. The results for the validation case are shown in Fig. 10. showing a graph for the coefficient of pressure along the horizontal wall of the inlet. Fig. 11 shows the geometry of validated case. Hence found that numerical solutions are matched with the experimental result.

A. Results for M4 Inlet

The post-processor result from analysis is drawn into a graph for all inlet geometry chosen from Table 4 for angles 10°,10.5°,10.75°, and 10.85°. Results are calibrated along the centre line of the isolator as shown in Figure14.Temperature, Mach number and static pressure along the centre line length graph are shown in Fig. 13-15. As we see from the results the values of temperature, Mach number and static pressure are converging as the angle is increased So, the geometry with an angle of 10.85° angle has matched with the required condition beyond increasing the angle, and the inlet gets unstarted because the shock which reflected back from cowl is propagating outside of isolator. From Table 6 it concluded that the error between the values is less than 4%. so, the inlet with a 10.85° is best for the M4 inlet. The contour of Mach number, pressure, and density for the M5 inlet with a 10.85° angle are shown in Fig. 16-18. Shock-on-lip condition is satisfied, all the shocks have impinged exactly at the cowl tip, and there is no flow spillage in inlet. The boundary layer at the vehicle forebody and ramp walls are thinner than the boundary layer at Mach. It is clearly visible that the shock train is propagating inside the isolator, so that pressure and temperature are increased and velocity is decreased at the end of the isolator due to flow passing through the continuous shock train. Fig. 19-20 represents the density and total pressure along the centreline of the isolator.

B. Results for M5 Inlet

All inlets geometry chosen from Table 5 for angles 10°,10.5°,11°, and 11.25°. Temperature, Mach number and static pressure along the centreline length graph are shown in Fig. 21-23. The geometry with an angle of 11.25° angle has matched with the required condition. From the Table 7, the error between the values is less than 4%. Temperature, Mach number and static pressure along the centre line length graph are shown in Fig.24-26. The shock-on-lip condition is satisfied, all the shocks have impinged exactly at the cowl tip.

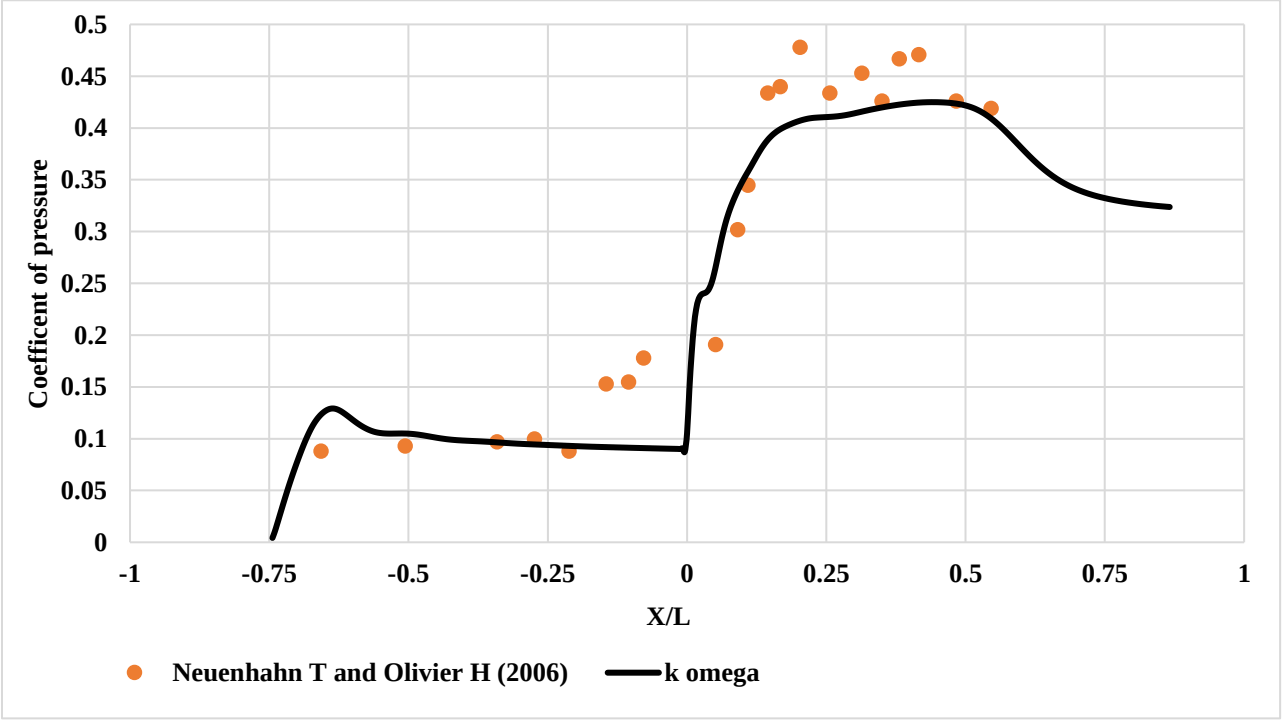

Fig. 10 Result of coefficient of pressure vs length

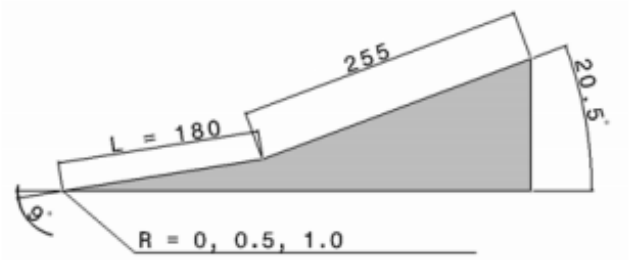

Fig. 11 Geometry of validated case

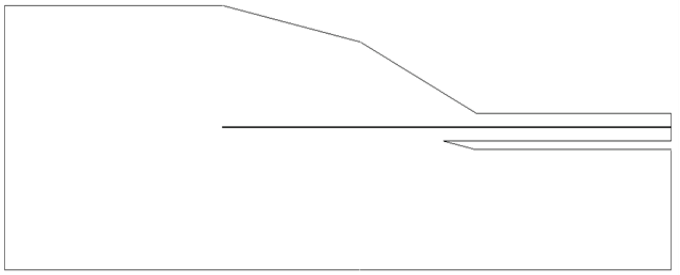

Fig. 12 Centreline location of geometry

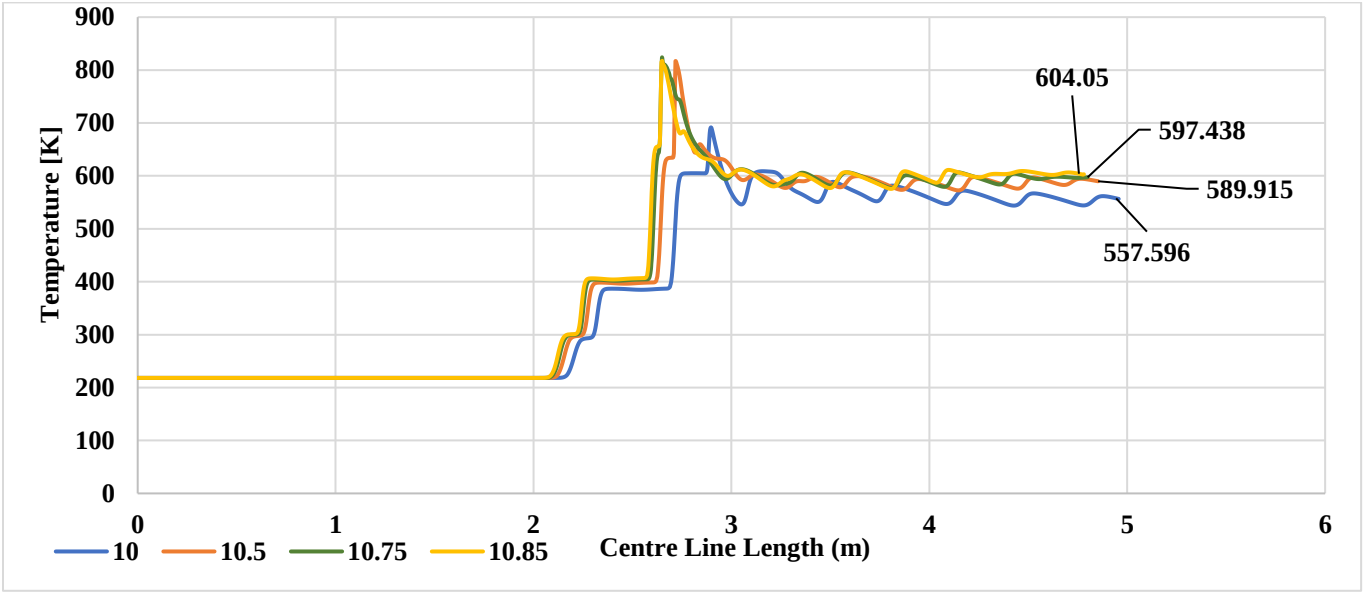

Fig. 13 Temperature along centreline of M4 inlets for different ramp angles

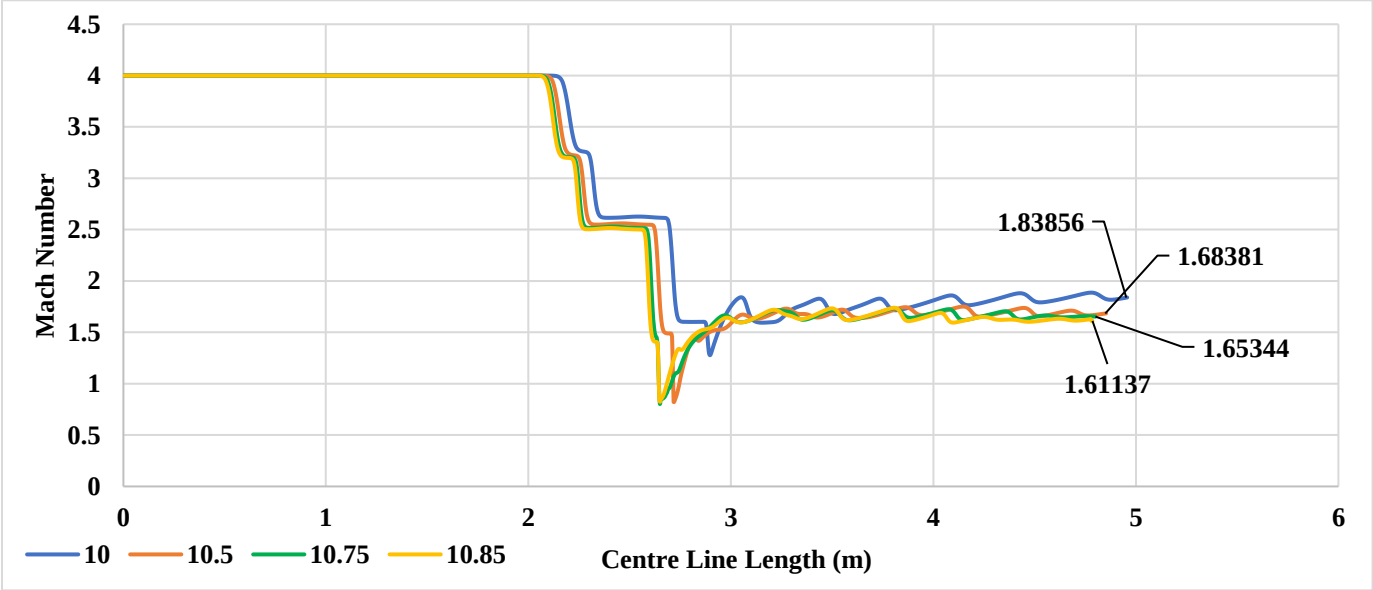

Fig. 14 Mach number along centreline of M4 inlets for different ramp angles

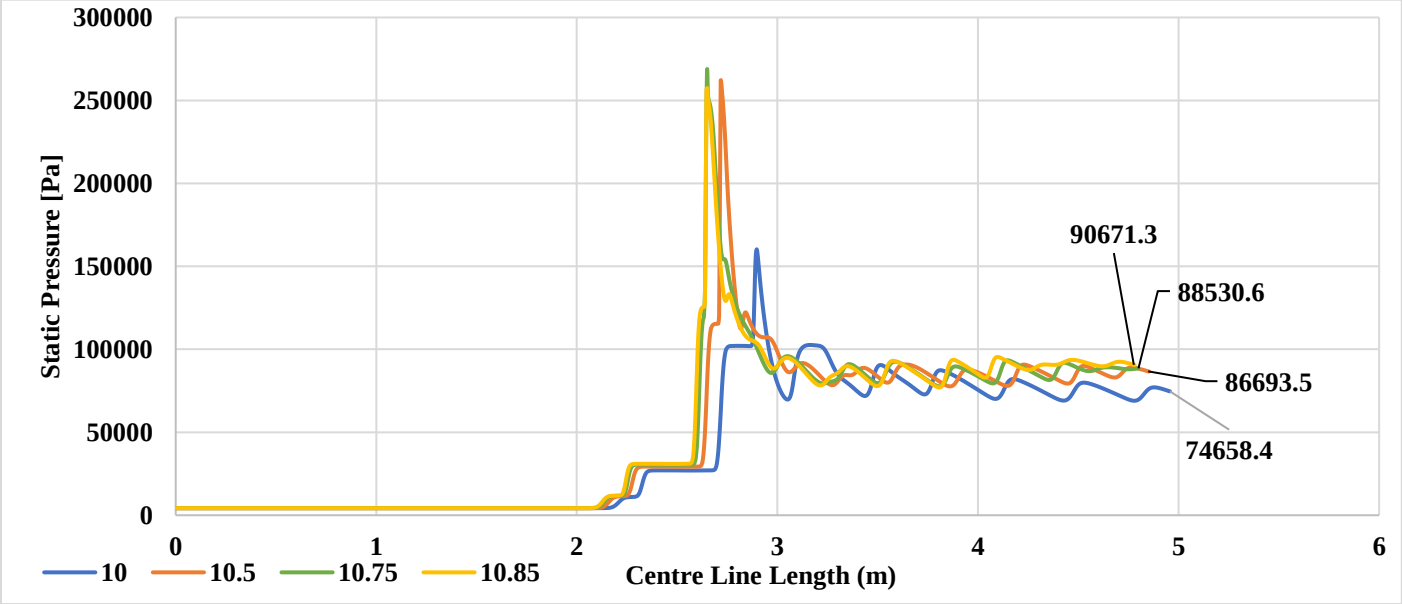

Fig. 15 Static pressure along centreline of M4 inlets for different ramp angles

Table 6. Comparison of results from CFD and required design results for M4 inlet

	Result Values	Required value	Percentage Error
Temperature (K)	604.05	611.016	1.1
Mach Number	1.61137	1.581	1.913
Pressure (N/m$^{2)}$	90671.3	87983.695	3.054

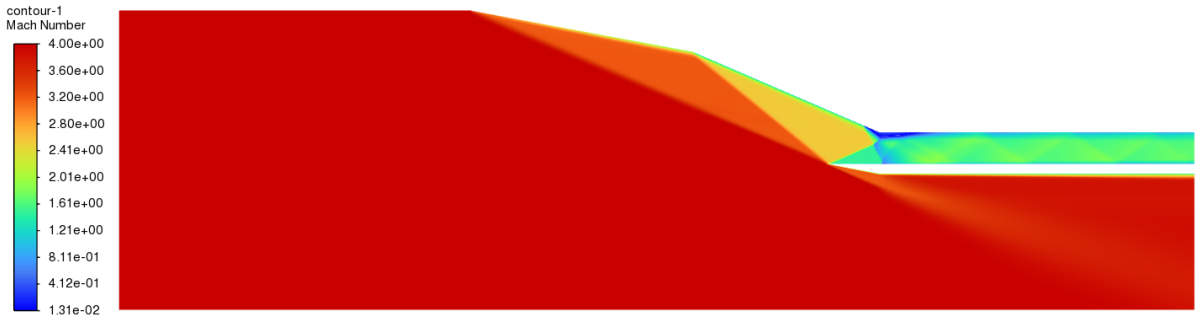

Fig. 16 Mach number contour for M4 inlet with 10.85° ramp angle

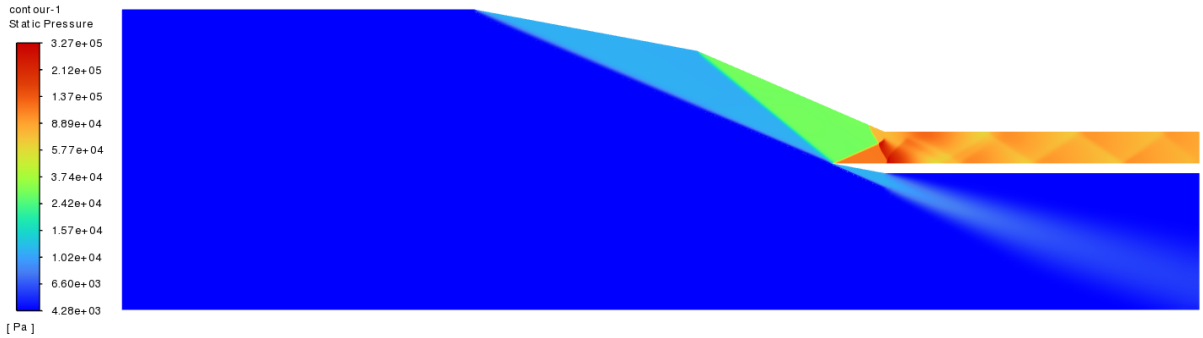

Fig. 17 Static pressure contour for M4 inlet with 10.85° ramp angle

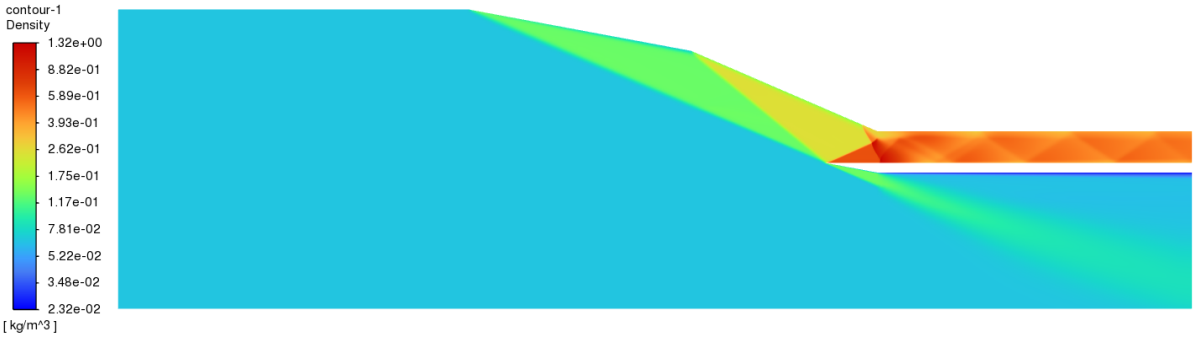

Fig. 18 Density contour for M4 inlet with 10.85° ramp angle

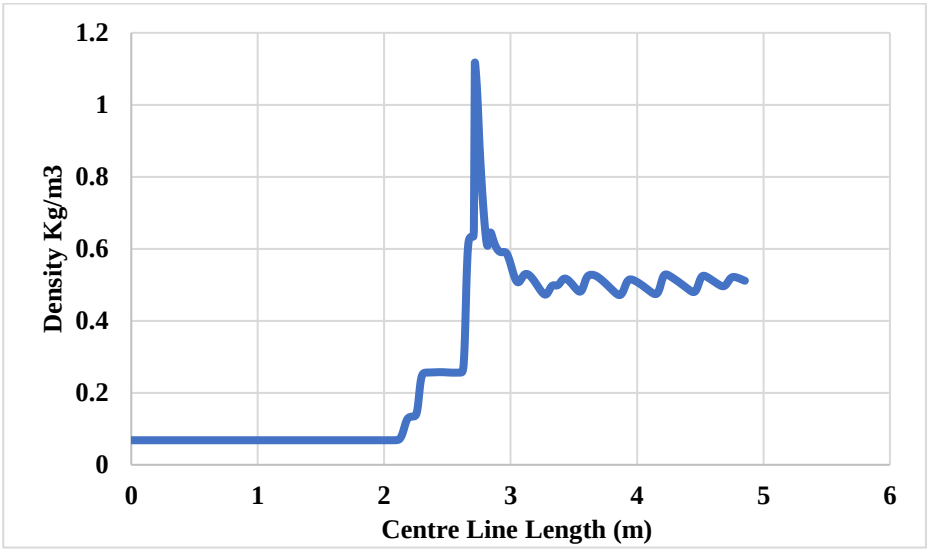

Fig. 19 Density along centreline for M4 inlet with 10.85° ramp angle

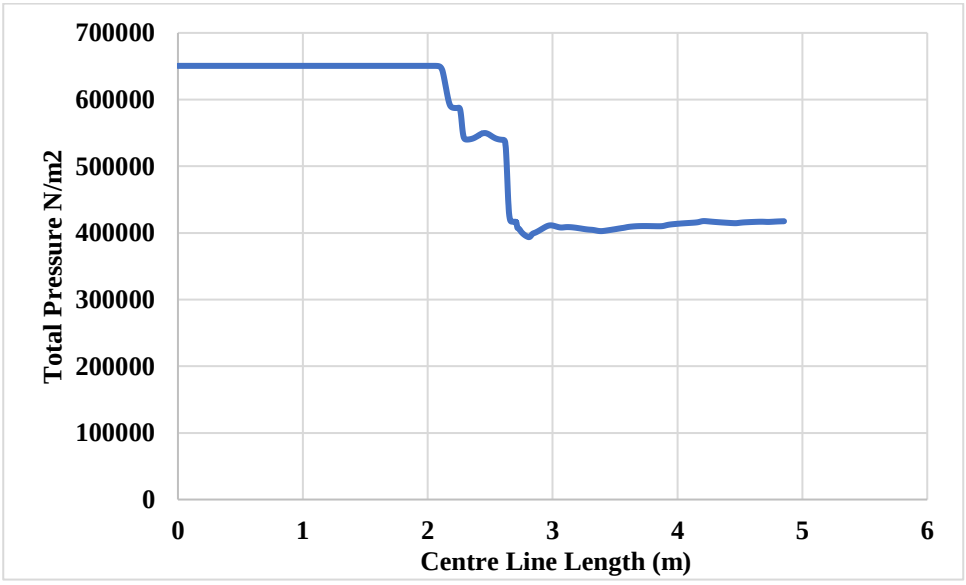

Fig. 20 Total pressure along centreline for M4 inlet with 10.85° ramp angle

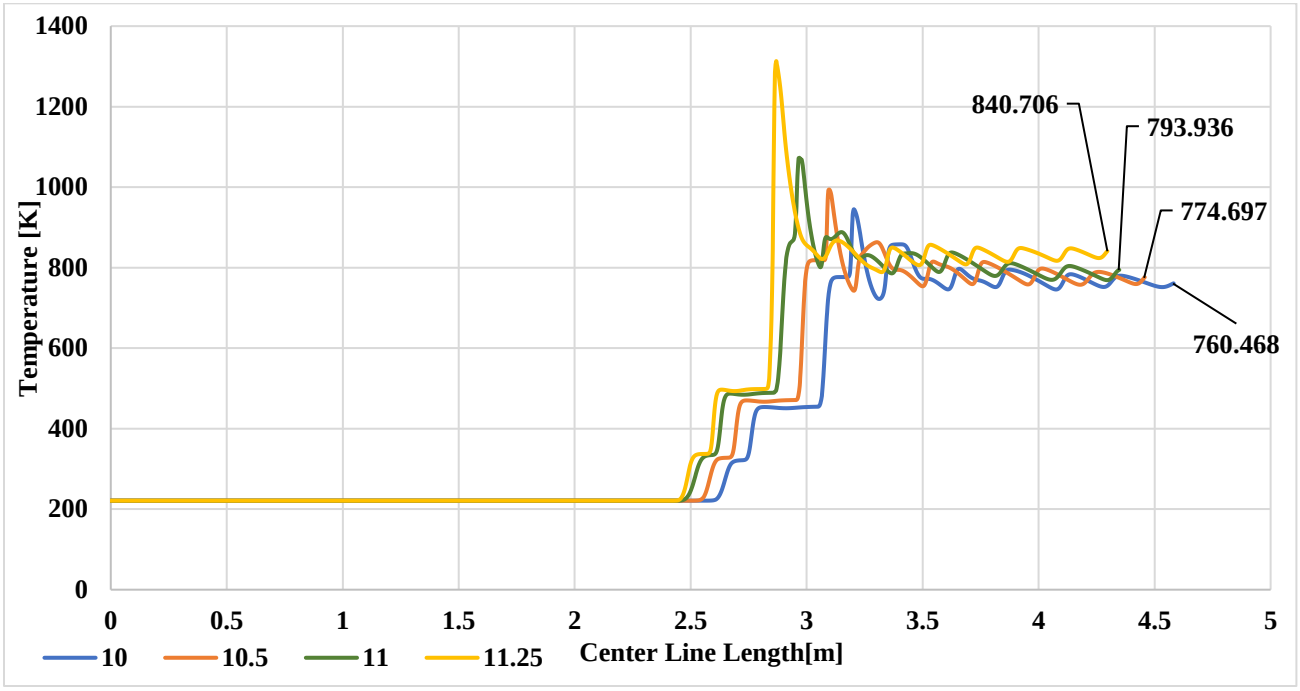

Fig. 21 Temperature along centreline of M5 inlets for different ramp angles

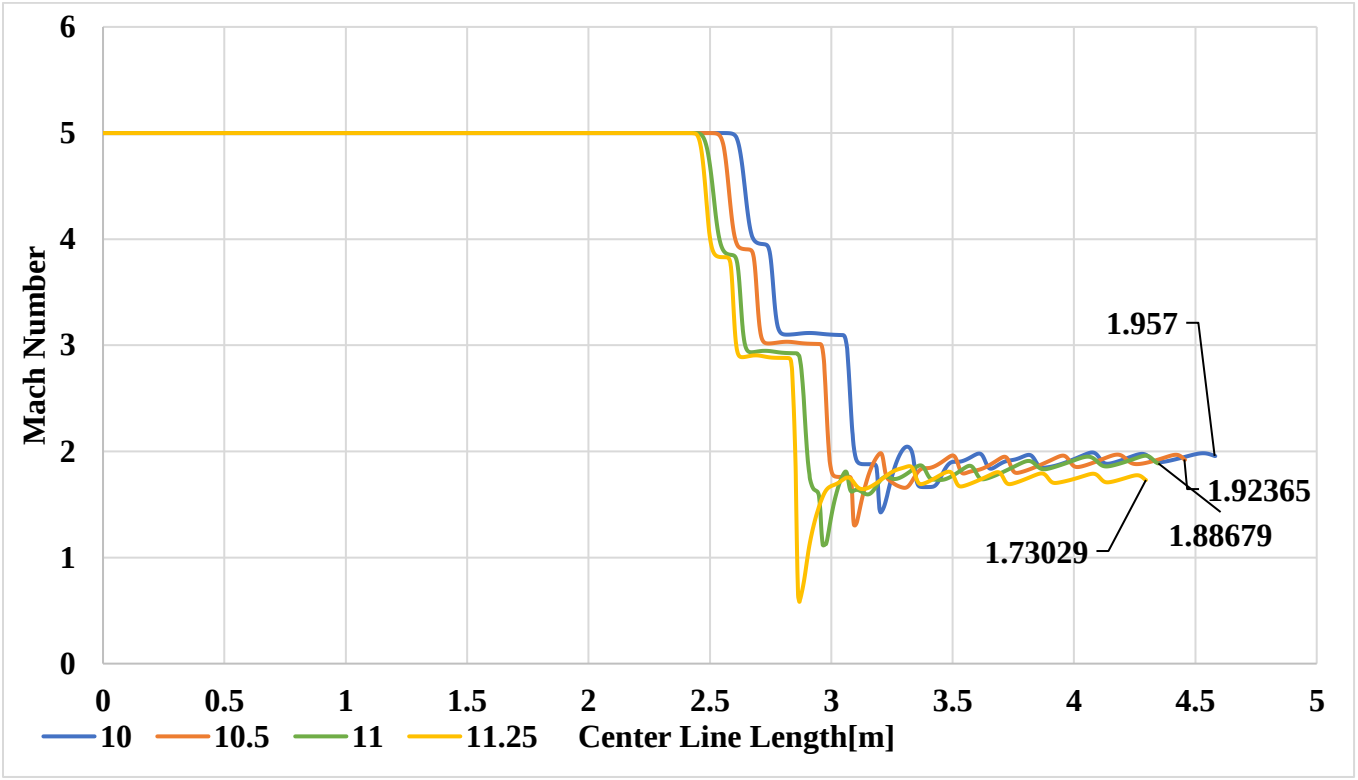

Fig. 22 Mach number along centreline of M5 inlets for different ramp angles

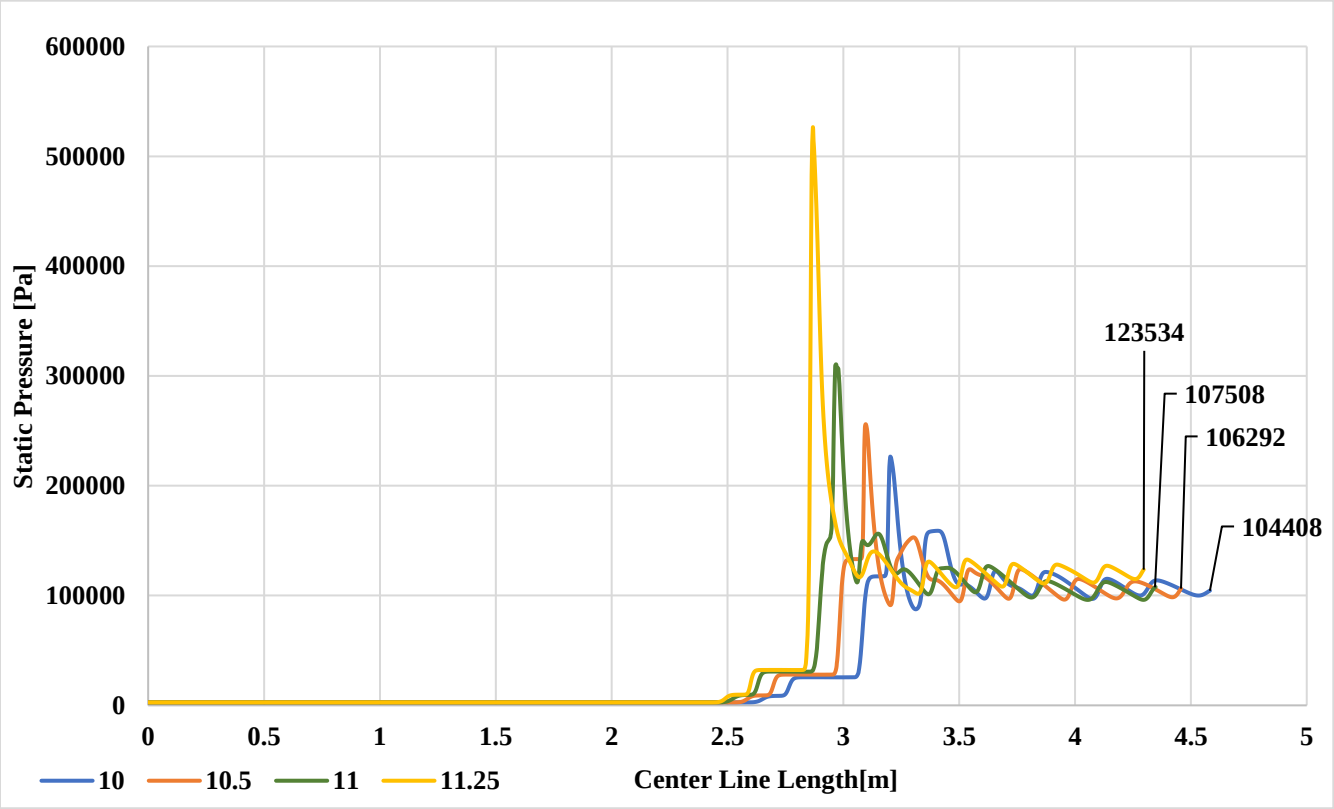

Fig. 23 Static pressure along centreline of M5 inlets for different ramp angles

Table 7. Comparison of results from CFD and required design results for M5 inlet

	Result Values	Required value	Percentage Error
Temperature (K)	840.706	829.087	1.401
Mach Number	1.730	1.732	0.115
Pressure (N/m$^{2)}$	123534	119382.281	3.477

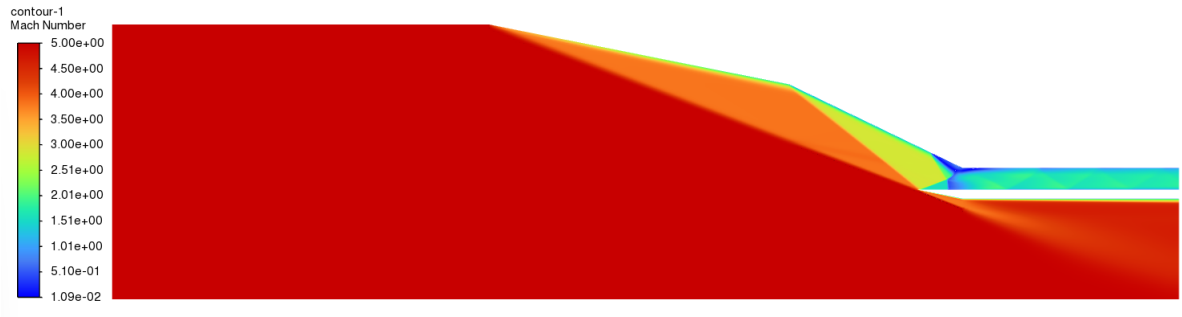

Fig. 24 Mach number contour for M5 inlet with 11.25° ramp angle

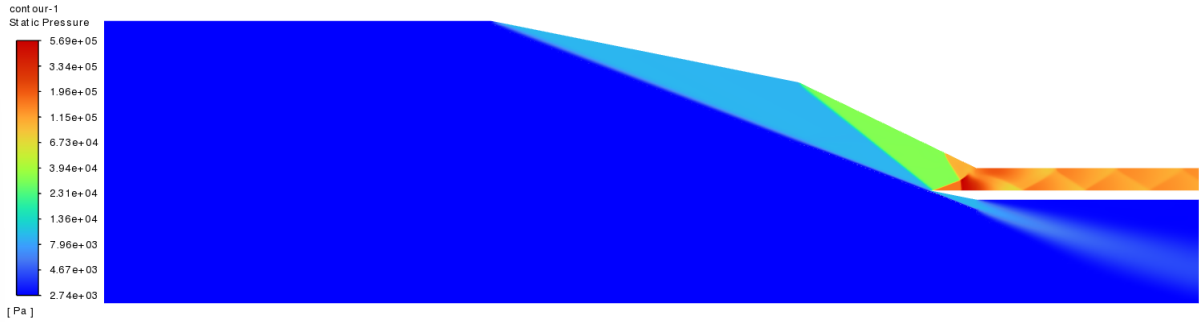

Fig. 25 Static pressure contour for M5 inlet with 11.25° ramp angle

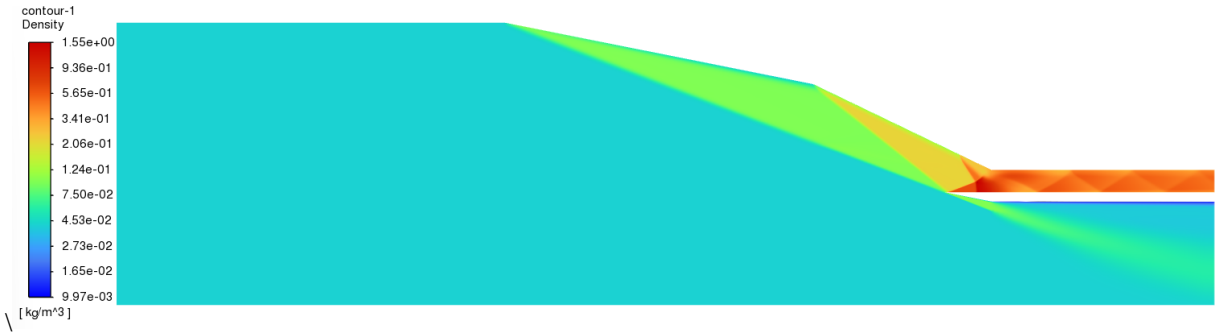

Fig. 26 Density contour for M5 inlet with 11.25° ramp angle

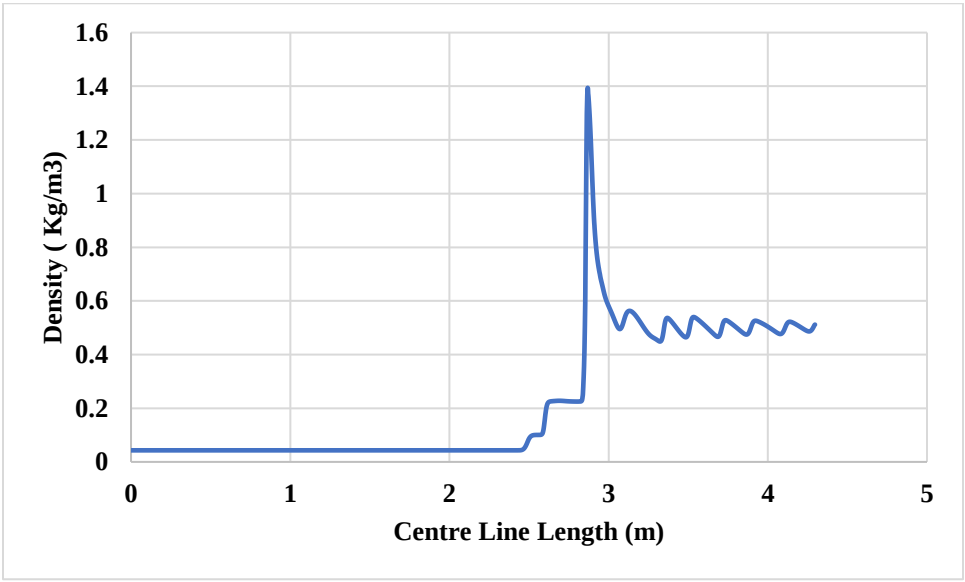

Fig. 27 Density along centreline for M5 inlet with 11.25° ramp angle

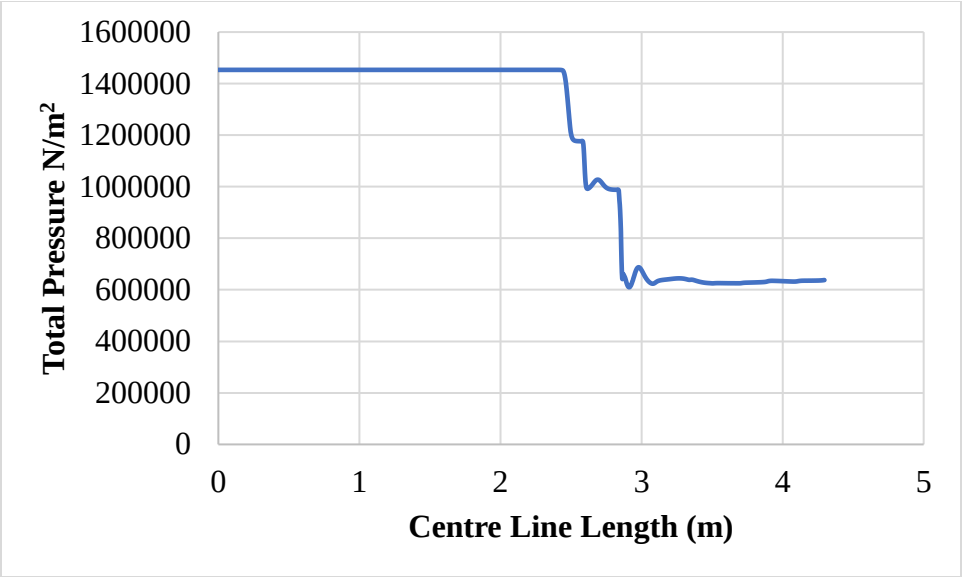

Fig. 28 Total pressure along centreline for M5 inlet with 11.25° ramp angle

IV. Conclusion

In this project, this project, for designing hypersonic intake geometry at Mach number 4 and 5 which are considered as low starting Mach numbers, so we have selected intake with 2 ramps and compression efficiency of 0.90. So, for different ramp angles, the geometry has been designed, to analyse which angle gives the result as our required condition as mentioned in section 3.2. the design constraints, computational domains, grid-independent checking and other factors were defined. And then, the results of Numerical solution were validated by experimental results of [14] and found good agreement. The software used for Numerical analysis is "Ansys Fluent 21 R2". we have designed Inlet for Mach number 4 with Ramp angles of 10°,10.5°,10.75°, and 10.85° and for Mach number 5 with ramp angles of 10°,10.5°,11°, and 11.25°. Post-processing of all the models was examined, by using the result of pressure, Mach number, and Temperature over the centreline of an isolator. We have found that results for the inlet with a ramp angle of 10.85° for M4 and inlet with a ramp angle of 11.25° for M5 have matched with the required condition for combustion in scramjet engine for low starting Mach number, shock-on-lip condition was also satisfied, as the shocks have impinged exactly at the cowl tip. There is no flow spillage happened in these cases. increasing the wedge angle beyond the limit angle we found that the shock reflected from the cowl is incident outside of the isolator causing the engine to unstart.

Nomenclature

A_0	Area of Entrance of Capture
A_3	Area of Entrance of Isolator
C_{pc}	Specific Heat for Engine Compression
CFD	Computational Fluid Dynamics
h_0	Height of Capture Area
h_3	Height of Isolator Area
IT	Ignition Temperature
l_c	Length of Cowl Isolator
l_o	Length of Isolator
l_I	Length of I Ramp
l_{II}	Length of II Ramp
M	Mach Number
M_0	Freestream Mach Number
M_3	Burner Entry Mach Number
p_0	Freestream Static Pressure
p_3	Static Pressure at Burner Entrance
q	Dynamic Pressure
R	Specific Gas Constant
S	Sutherland Temperature
T	Temperature
T_{ref}	Reference Temperature
T_0	Free Stream Static Temperature
T_3	Static Temperature at Burner Entrance
V_0	Freestream Velocity
V_3	Velocity at Burner Entrance
β_I	Shock Angle Generated by I Ramp
β_{II}	Shock Angle Generated by II Ramp
γ_c	Ratio of Specific Heats for Compression

η_c	Inlet Compression System Efficiency
μ	Dynamic Viscosity
μ_{ref}	Viscosity at Reference Temperature
ρ	Density
2D	Two Dimensional

REFERENCES

[1] Sen, D., Pesyridis, A., & Lenton, A. (2018). A scramjet compression system for hypersonic air transportation vehicle combined cycle engines. *Energies*, *11*(6), 1568.

[2] Heiser, W. H., Pratt, D. T., & Daley, D. H. (1994). *Hypersonic airbreathing propulsion*. Aiaa.

[3] Smart, M. K. (2010). *Scramjet inlets*. QUEENSLAND UNIV BRISBANE (AUSTRALIA) CENTRE FOR HYPERSONICS.

[4] Fry, R. S. (2004). A century of ramjet propulsion technology evolution. *Journal of propulsion and power*, *20*(1), 27-58..

[5] Anderson, J. D. (1990). *Modern compressible flow: with historical perspective* (Vol. 12). New York: McGraw-Hill.

[6] Oswatitsch, K. (1980). Pressure recovery for missiles with reaction propulsion at high supersonic speeds (the efficiency of shock diffusers). In *Contributions to the Development of Gasdynamics* (pp. 290-323). Vieweg+ Teubner Verlag.

[7] Raj, N. O. P., & Venkatasubbaiah, K. (2012). A new approach for the design of hypersonic scramjet inlets. *Physics of Fluids*, *24*(8), 086103.

[8] Araújo, P. P., Pereira, M. V., Marinho, G. S., Martos, J. F., & Toro, P. G. (2021). Optimization of scramjet inlet based on temperature and Mach number of supersonic combustion. *Aerospace Science and Technology*, *116*, 106864.

[9] Roberts, K., & Wilson, D. (2009, January). Analysis and design of a hypersonic scramjet engine with a transition Mach number of 4.00. In *47th AIAA aerospace sciences meeting including the new horizons forum and aerospace exposition* (p. 1255).

[10] Karthikeyan, P., Prakash, B., & Balakrishnan, S. R. Effect Of Inlet Performance And Starting Mach Number On The Design Of A Scramjet Engine.

[11] Zore, K., Ozcer, I., Munholand, L., & Stokes, J. ANSYS CFD Simulations of Supersonic and Hypersonic Flows.

[12] Gollan, R., Gollan, R., Ferlemann, P., & Ferlemann, P. (2011, April). Investigation of REST-class hypersonic inlet designs. In *17th AIAA International Space Planes and Hypersonic Systems and Technologies Conference* (p. 2254).

[13] Sutherland, W. (1893). LII. The viscosity of gases and molecular force. *The London, Edinburgh, and Dublin Philosophical Magazine and Journal of Science*, *36*(223), 507-531.

[14] Neuenhahn, T., & Olivier, H. (2006). Influence of the wall temperature and the entropy layer effects on double wedge shock boundary layer interactions. In *14th AIAA/AHI space planes and hypersonic systems and technologies conference* (p. 8136).